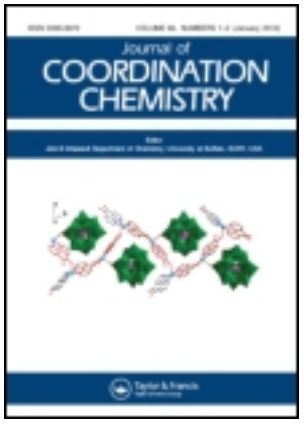

Journal of Coordination Chemistry
Publication details, including instructions for authors and subscription information:
http://www.tandfonline.com/loi/gcoo20

Synthesis, characterization, DNA-binding, and antioxidant activities of four copper(II) complexes containing N-(3-hydroxybenzyl)-amino amide ligands

ZHI Li- HUA [a] , WU WEI- NA [a] , WANG YUAN [a] & SUN GUANG [b]
[a] Department of Physics and Chemistry , Henan Polytechnic University , Jiaozuo , PR , China
[b] School of Materials Science and Engineering , Henan Polytechnic University , Jiaozuo , PR , China
Accepted author version posted online: 28 Nov 2012.Published online: 14 Jan 2013.

To cite this article: ZHI Li- HUA , WU WEI- NA , WANG YUAN & SUN GUANG (2013) Synthesis, characterization, DNA-binding, and antioxidant activities of four copper(II) complexes containing N-(3-hydroxybenzyl)-amino amide ligands, Journal of Coordination Chemistry, 66:2, 227-242, DOI: 10.1080/00958972.2012.754018

To link to this article: http://dx.doi.org/10.1080/00958972.2012.754018

Journal of Coordination Chemistry
Vol. 66, No. 2, 20 January 2013, 227–242

Synthesis, characterization, DNA-binding, and antioxidant activities of four copper(II) complexes containing N-(3-hydroxybenzyl)-amino amide ligands

ZHI LI- HUA†, WU WEI- NA†*, WANG YUAN† and SUN GUANG‡

†Department of Physics and Chemistry, Henan Polytechnic University, Jiaozuo, PR, China; ‡School of Materials Science and Engineering, Henan Polytechnic University, Jiaozuo, PR, China

(*Received 20 May 2012; in final form 1 October 2012*)

Four new substituted amino acid ligands, N-(3-hydroxybenzyl)-glycine acid (HL_1), N-(3-hydroxybenzyl)-alanine acid (HL_2), N-(3-hydroxybenzyl)-phenylalanine acid (HL_3), and N-(3-hydroxybenzyl)-leucine acid (HL_4), were synthesized and characterized on the basis of ^{1}H NMR, IR, ESI-MS, and elemental analyses. The crystal structures of their copper(II) complexes $[Cu(L_1)_2]\cdot 2H_2O$ (**1**), $[Cu(L_2)_2(H_2O)]$ (**2**), $[Cu(L_3)_2(CH_3OH)]$ (**3**), and $[Cu(L_4)_2(H_2O)]\cdot H_2O$ (**4**) were determined by X-ray diffraction analysis. The ligands coordinate with copper(II) through secondary amine and carboxylate in all complexes. In **2**, **3,** and **4**, additional water or methanol coordinates, completing a distorted tetragonal pyramidal coordination geometry around copper. Fluorescence titration spectra, electronic absorption titration spectra, and EB displacement indicate that all the complexes bind to CT-DNA. Intrinsic binding constants of the copper(II) complexes with CT-DNA are $1.32 \times 10^6\,M^{-1}$, $4.32 \times 10^5\,M^{-1}$, $5.00 \times 10^5\,M^{-1}$, and $5.70 \times 10^4\,M^{-1}$ for **1**, **2**, **3,** and **4**, respectively. Antioxidant activities of the compounds have been investigated by spectrophotometric measurements. The results show that the Cu(II) complexes have similar superoxide dismutase activity to that of native Cu, Zn-SOD.

Keywords: Substituted amino acid ligand; Copper(II) complex; Crystal structure; DNA Binding; Antioxidant activity

1. Introduction

There has been increasing focus on binding of small molecules to DNA, since DNA contains all the genetic information for cellular functions [1–3]. DNA molecules are prone to damage by interacting with some chemicals. This damage may change the replication of DNA and inhibit the growth of tumor cells in living organisms, which is the basis of designing more efficient antitumor drugs [4–6].

Amino acids are basic structural units of proteins and play central roles both as building blocks of proteins and as intermediates in metabolism. Amino acid Schiff bases have been used as ligands in coordination chemistry [7]. Several metal complexes of Schiff bases derived from salicylaldehyde and amino acid [8–11] were reported; some have been

*Corresponding author. Email: wuwn08@hpu.edu.cn

ISSN 0095-8972 print/ISSN 1029-0389 online © 2012 Taylor & Francis
http://dx.doi.org/10.1080/00958972.2012.754018

proven to be efficient DNA cleavers [12,13] and as novel tumor chemotherapeutic and tumor radio imaging agents [14]. Copper(II) complexes containing amino acids have attracted attention for their biological and pharmaceutical activities and studied as models for the behavior of copper enzymes. Some copper complexes with amino acid ligands were reported to exhibit potent antitumor and artificial nuclease activities [15–17]. Recent reports have also shown that amino acid/peptide based copper(II) complexes show efficient DNA cleavage activity [18–20].

Four new Cu(II) complexes with amino acid ligands (figure 1) were synthesized and characterized. DNA-binding properties of the complexes have been investigated by UV absorption and fluorescence spectroscopy as well as their antioxidant activities *in vitro*. These results help to understand the binding mode of this kind of complex to DNA, useful to explore new anticancer agents and antioxidants, and to modify or detect bio-molecules.

2. Experimental

2.1. *Materials and instrumentation*

All chemicals were of analytical grade and used without purification unless otherwise noted. All measurements involving interactions of the four metal complexes with CT-DNA were carried out in doubly distilled water buffer. UV–Vis spectrometry was employed to check the solution concentration of CT-DNA ($\varepsilon = 6600\,M^{-1}\,cm^{-1}$ at 260 nm) and the purity (A260:A280 > 1.80) in the buffer. UV–Vis absorption spectra were recorded using a Purkinje General TU-1901 spectrophotometer and fluorescence emission spectra were recorded using a Varian CARY Eclipse spectrofluorophotometer. Melting points were determined on an XT4-100× microscopic melting point apparatus (Beijing Electrooptical Instrument Factory, China). Elemental analyses for C, H, and N were carried out on an Elemental Vario EL analyzer. IR spectra ($v = 4000$–$400\,cm^{-1}$) were determined by the KBr

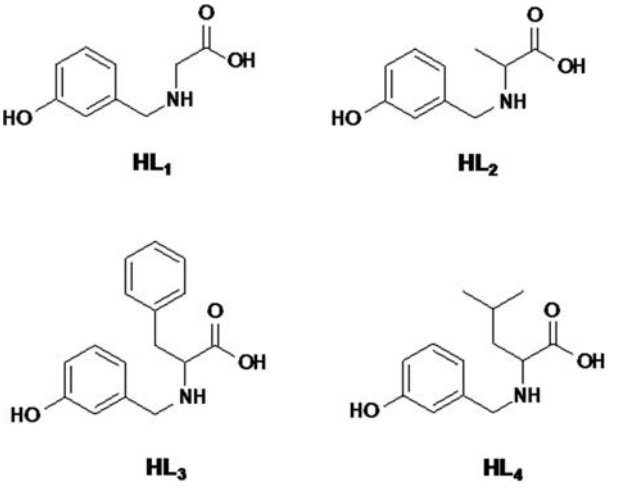

Figure 1. The structure of the ligands.

pressed disk method on a Bruker V70 FT-IR spectrometer. ^{1}H NMR spectra were recorded with a Bruker AV400 NMR instrument using appropriate deuterated solvents. ESI mass spectra were recorded on a Finnigan MAT LCQ mass spectrometer using the syringe pump method. Antioxidant activities were tested on a 722 N spectrophotometer (Shanghai Analytical Instrument Factory, China).

2.2. *Synthesis of the ligands*

All ligands were synthesized by reducing the Schiff base formed from the corresponding amino acid and 3-hydroxy benzaldehyde via $NaBH_4$ according to the literature [21].

HL_1: Yield: 66%. m.p. 215–216 °C. Anal. Calcd for $C_9H_{11}NO_3$: C, 59.66; H, 6.12; N, 7.73. Found: C, 59.37; H, 5.86; N, 7.48%. ESI-MS Calcd. for $C_9H_{11}NO_3$: 181.07. Found: 182.1. ^{1}H NMR (D_2O) δ 1.93 (s, 1H, −NH), 3.63 (s, 2H, $-CH_2-$), 4.22 (s, 1H, −OH), 6.98–7.06 (*m*, 3H, C−H, phen), 7.36–7.41 (m, 1H, C−H, phen). IR (KBr, cm^{-1}): υ(NH) 3104; υ(CH_2) 2889; υ(COO^-) 1605, 1382; υ(OH) 3416.

HL_2: Yield: 62%. m.p. 245–247 °C. Anal. Calcd for $C_{10}H_{13}NO_3$: C, 61.53; H, 6.71; N, 7.18. Found: C, 61.25; H, 6.43; N, 6.9%. ESI-MS Calcd. for $C_{10}H_{13}NO_3$: 195.09. Found: 196.1. ^{1}H NMR (D_2O) δ 1.51 (s, 3H, CH_3), 1.93 (s, 1H, NH), 3.72 (p, 1H, CH), 4.22 (d, 2H, CH_2),7.04 (m, 3H, CH, phen), 7.38(t, 1H, CH, phen). IR (KBr, cm^{-1}): υ(NH) 3150; υ(CH_2) 2990; υ(COO^-) 1611, 1414; υ(OH) 3433.

HL_3: Yield: 58%. m.p. 229–231 °C. Anal. Calcd for $C_{16}H_{17}NO_3$: C, 70.83; H, 6.32; N, 5.16. Found: C, 70.56; H, 6.14; N, 4.88%. ESI-MS Calcd. for $C_{16}H_{17}NO_3$: 271.12. Found: 272.2. ^{1}H NMR (MeOD) δ 1.88 (s, 1H, NH), 3.02–3.27 (m, 2H, CH_2), 3.66–3.69 (d, 2H, CH_2), 3.89–3.99 (t, 1H, CH), 4.8 (s, 1H, OH), 6.75–6.78 (t, 3H, CH, phen), 7.14–7.18 (t, 1H, CH, phen), 7.21–7.27 (m, 5H, CH, phen). IR (KBr, cm^{-1}): υ(NH) 3088; υ(CH_2) 2949; υ(COO^-) 1632, 1390; υ(OH) 3180.

HL_4: Yield: 68%. m.p. 179–183 °C. Anal. Calcd for $C_{13}H_{19}NO_3$: C, 65.8; H, 8.07; N, 5.9. Found: C, 65.57; H, 8.26; N, 5.64%. ESI-MS Calcd. for $C_{13}H_{19}NO_3$: 237.29. Found: 238.3. ^{1}H NMR (D_2O) δ 0.62–0.75 (m, 6H, CH_3), 1.37–1.49 (m, 3H, CH, CH_2), 1.69 (s, 1H, NH), 3.29–3.52 (t, 1H, CH), 3.81–3.97 (d, 2H, CH), 6.75–6.78 (m, 3H, CH, phen), 7.06–7.14 (t, 1H, CH, phen) cm. IR (KBr, cm^{-1}): υ(NH) 3061; υ(CH_2) 2960; υ(COO^-) 1610, 1408; υ(OH) 3443.

2.3. *Synthesis of the complexes*

All complexes were synthesized using a similar method according to the literature [21]. **1** and **2** were obtained from water solutions. However, **3** and **4** were obtained from MeOH/H_2O (2:3) solution.

1: Yield: 82%. Anal. Calcd for $C_{18}H_{24}CuN_2O_8$: C, 47.00; H, 5.26; N, 6.09. Found: C, 46.72; H, 4.97; N, 5.83%. IR (KBr, cm^{-1}): υ(NH) 2970; υ(CH_2) 2939; υ(COO^-) 1593, 1402; υ(H_2O and/or OH) 3423, 3269.

2: Yield: 78%. Anal. Calcd for $C_{20}H_{26}CuN_2O_7$: C, 51.11; H, 5.58; N, 5.96. Found: C, 50.84; H, 5.30; N, 5.68%. IR (KBr, cm^{-1}): υ(NH) 3076; υ(CH_2) 2966; υ(COO^-) 1604, 1479; υ(H_2O and/or OH) 3425, 3215.

3: Yield: 87%. Anal. Calcd for $C_{33}H_{36}CuN_2O_7$: C, 62.30; H, 5.70; N, 4.40. Found: C, 62.05; H, 5.44; N, 4.12%. IR (KBr, cm^{-1}): υ(NH) 3028; υ(CH_2) 2929; υ(COO^-) 1649, 1427; υ(OH) 3279, 3223.

4: Yield: 75%. Anal. Calcd for $C_{26}H_{40}CuN_2O_8$: C, 54.58; H, 7.05; N, 4.90. Found: C, 54.61; H, 7.27; N, 4.73%. IR (KBr, cm^{-1}): υ(NH) 3271; υ(CH_2) 2960; υ(COO^-) 1616, 1465; υ(OH) 3421, 3298.

2.4. *X-ray Crystallography*

The crystals were mounted on a Bruker SMART APEX II CCD diffractometer equipped with a graphite monochromated Mo-*K*α radiation ($\lambda = 0.071073$ nm) by using ϕ–ω scan mode. SMART [22] was used to collect the intensity data, SAINT for integration of the intensity [22], SADABS [23] for absorption correction, and SHELXTL [24] for structure solution and refinements on F^2. A summary of the crystal data is given in table 1. Selected bond angles and distances are listed in table 2. The details of the hydrogen bond parameters are given in table 3.

2.5. *Spectroscopic studies on DNA interaction*

2.5.1. Electronic absorption spectra. Electronic absorption titration of copper(II) complexes in aqueous buffer solution (50 mM NaCl–5 mM Tris-HCl, pH 7.1) were performed at a fixed complex concentration (10 μM) while gradually increasing the concentration of CT-DNA. Absorption data were analyzed to evaluate the intrinsic binding constant K_b, which can be determined from equation (1) [25],

$$[\mathrm{DNA}]/(\varepsilon_a - \varepsilon_f) = [\mathrm{DNA}]/(\varepsilon_b - \varepsilon_f) + 1/[K_b(\varepsilon_b - \varepsilon_f)] \quad (1)$$

where, [DNA] is the concentration of DNA in base pairs; ε_a, ε_f, and ε_b are the apparent extinction coefficient (A_{obsd}/[compound]), the extinction coefficient for the free compound and the extinction coefficient for the compound in the fully bound form, respectively. A plot of $[\mathrm{DNA}]/(\varepsilon_b - \varepsilon_f)$ *vs.* [DNA] gave a slope of $1/(\varepsilon_b - \varepsilon_f)$ and an intercept equal to $[K_b(\varepsilon_b - \varepsilon_f)]^{-1}$; K_b is the ratio of the slope to the intercept.

2.5.2. Fluorescence spectra. *Fluorescence spectral titration.* For fluorescence measurements, fixed concentrations (10 μM) of the complexes were titrated with increasing amounts of CT-DNA. The excitation and emission wavelengths were 275.2 and 302.96 for **1** and 274 and 302 for **2**, **3,** and **4**. Excitation and emission slits were set at 5 nm. Experiments were conducted at room temperature in a buffer containing 5 mM Tris-HCl (pH 7.1) and 50 mM NaCl.

EB–DNA competition experiment. Further support for the binding mode of the four complexes to DNA is given through emission quenching experiments. A 2 mL solution of 30 μM CT-DNA and 2 μM EB was titrated by small aliquots of concentrated compound solutions until the drop in fluorescence intensity (Ex = 500 nm, Em = 520.0–720.0 nm) attained saturation. Measurements were made at constant room temperature in Tris-HCl buffer solution. Quenching data were analyzed according to the Stern–Volmer equation (2) which could be used to determine the fluorescent quenching mechanism [26]:

Table 1. Selected crystallographic data for **1**–**4**.

Compound	**1**	**2**	**3**	**4**
Empirical formula	$C_{18}H_{24}CuN_2O_8$	$C_{20}H_{26}CuN_2O_7$	$C_{33}H_{35}CuN_2O_7$	$C_{26}H_{40}CuN_2O_8$
Formula weight	459.93	469.97	635.17	572.14
Temperature (K)	296(2)	296(2)	296(2)	296(2)
Crystal system	Triclinic	Orthorhombic	Orthorhombic	Orthorhombic
Space group	*P*-1	$P2_12_12_1$	$P2_12_12_1$	$P2_12_12_1$
a (Å)	6.44520(10)	10.1848(7)	6.9144(6)	9.9210(12)
b (Å)	7.58580(10)	10.2319(7)	14.0569(13)	11.1061(14)
c (Å)	10.76830(10)	19.8301(13)	32.007(3)	26.989(3)
α (°)	82.2090(10)	90	90	90
β (°)	75.5290(10)	90	90	90
γ (°)	72.2930(10)	90	90	90
V (Å^3)	484.616(11)	2066.5(2)	3110.9(5)	2973.7(6)
Z	1	4	4	4
Calculated density (Mg/m^3)	1.576	1.511	1.356	1.278
Absorption coefficient (mm^{-1})	1.176	1.102	0.752	0.781
F(000)	239	980	1328	1212
Crystal size (mm)	0.18 × 0.15 × 0.10	0.22 × 0.20 × 0.15	0.23 × 0.20 × 0.18	0.21 × 0.18 × 0.17
θ range (°)	2.82–30.35	2.05–28.40	1.93–27.85	1.98–28.11
Limiting indices	$-9 \leqslant h \leqslant 9$	$-13 \leqslant h \leqslant 13$	$-9 \leqslant h \leqslant 9$	$-13 \leqslant h \leqslant 11$
	$-10 \leqslant k \leqslant 10$	$-13 \leqslant k \leqslant 13$	$-17 \leqslant k \leqslant 16$	$-13 \leqslant k \leqslant 14$
	$-15 \leqslant l \leqslant 15$	$-26 \leqslant l \leqslant 15$	$-29 \leqslant l \leqslant 42$	$-32 \leqslant l \leqslant 35$
Reflections collected/unique	9651/2852 (R_{int} = 0.0210)	13374/4997 (R_{int} = 0.0299)	19697/7247 (R_{int} = 0.0414)	18926/7056 (R_{int} = 0.0541)
Refinement method	Full-matrix least-squares on F^2	Full-matrix least-squares on F^2	Full-matrix least-squares on F^2	Full-matrix least-squares on F^2
Data/restraints/parameters	2852/4/139	4997/3/274	7247/0/388	7056/185/350
Goodness-of-fit on F^2	1.040	1.008	1.078	1.086
Final R indices ($I > 2\sigma(I)$)	R_1 = 0.0538	R_1 = 0.0274	R_1 = 0.0418	R_1 = 0.0632
	wR_2 = 0.1321	wR_2 = 0.0601	wR_2 = 0.0849	wR_2 = 0.1475
R indices (all data)	R_1 = 0.0685	R_1 = 0.0336	R_1 = 0.0590	R_1 = 0.1131
	wR_2 = 0.1407	wR_2 = 0.0621	wR_2 = 0.0900	wR_2 = 0.1686
Largest diff. peak/hole (e Å^{-3})	0.658/−0.802	0.236/−0.325	0.650/−0.322	1.044/−0.491

Table 2. Selected bond lengths (Å) and angles (°) for **1**–**4**.

1					
Cu(1)–O(1)^{i}	1.933(2)	Cu(1)–O(1)	1.933(2)	O(1)^{i}–Cu(1)–O(1)	180.00(10)
Cu(1)–N(1)	2.011(3)	Cu(1)–N(1) ^{i}	2.011(3)	O(1)^{i}–Cu(1)–N(1)	95.50(10)
O(1)–Cu(1)–N(1)	84.50(10)	O(1)^{i}–Cu(1)–N(1)^{i}	84.50(10)	O(1)–Cu(1)-N(1)^{i}	95.50(10)
N(1)–Cu(1)–N(1)^{i}	180.0(2)	C(1)–O(1)–Cu(1)	115.65(18)		
2					
Cu(1)–O(2)	1.9274(14)	Cu(1)–O(5)	1.9423(13)	Cu(1)–N(1)	2.0211(15)
Cu(1)–N(2)	2.0239(15)	Cu(1)–O(7)	2.2834(14)	O(2)–Cu(1)–O(5)	171.54(6)
O(2)–Cu(1)–N(1)	85.00(6)	O(5)–Cu(1)–N(1)	96.53(6)	O(2)–Cu(1)–N(2)	92.12(6)
O(5)–Cu(1)–N(2)	84.56(6)	N(1)–Cu(1)–N(2)	167.14(6)	O(2)–Cu(1)–O(7)	90.84(6)
O(5)–Cu(1)–O(7)	97.25(6)	N(1)–Cu(1)–O(7)	96.35(6)	N(2)–Cu(1)–O(7)	96.22(6)
C(8)–N(1)–Cu(1)	107.52(11)	C(7)–N(1)–Cu(1)	113.68(12)	C(20)–O(5)–Cu(1)	115.82(12)
C(17)–N(2)–Cu(1)	109.35(12)	C(18)–N(2)–Cu(1)	108.56(11)	C(10)–O(2)–Cu(1)	116.05(13)
3					
Cu(1)–O(5)	1.9157(19)	Cu(1)–O(2)	1.9464(18)	Cu(1)–N(2)	2.0077(19)
Cu(1)–N(1)	2.0219(19)	Cu(1)–O(7)	2.295(2)	O(5)–Cu(1)–O(2)	172.75(9)
O(5)–Cu(1)–N(2)	93.17(8)	O(2)–Cu(1)–N(2)	83.44(9)	O(5)–Cu(1)–N(1)	84.79(8)
O(2)–Cu(1)–N(1)	95.72(8)	N(2)–Cu(1)–N(1)	156.15(9)	O(5)–Cu(1)–O(7)	94.00(8)
O(2)–Cu(1)–O(7)	93.05(9)	N(2)–Cu(1)–O(7)	104.48(9)	N(1)–Cu(1)–O(7)	99.37(9)
C(25)–O(2)–Cu(1)	115.67(17)	C(9)–O(5)–Cu(1)	108.12(15)	C(8)–N(1)–Cu(1)	106.44(15)
C(24)–N(2)–Cu(1)	108.31(15)	C(23)–N(2)–Cu(1)	105.73(15)		
4					
Cu(1)–O(2)	1.903(3)	Cu(1)–O(5)	1.940(4)	Cu(1)–N(2)	2.005(4)
Cu(1)–N(1)	2.017(4)	Cu(1)–O(7)	2.271(4)	O(2)–Cu(1)–O(5)	174.09(17)
O(2)–Cu(1)–N(2)	93.31(14)	O(5)–Cu(1)–N(2)	83.44(16)	O(2)–Cu(1)–N(1)	85.47(16)
O(5)–Cu(1)–N(1)	95.52(16)	N(2)–Cu(1)–N(1)	156.34(17)	O(2)–Cu(1)–O(7)	92.15(17)
O(5)–Cu(1)–O(7)	93.39(18)	N(2)–Cu(1)–O(7)	102.98(17)	N(1)–Cu(1)–O(7)	100.68(18)

Symmetry codes: (i) $-x+1$; $-y$, $-z$

Table 3. Main intra and intermolecular hydrogen bonds for **1**–**4** in this study (Å).

D–H···A	d(D–H)	d(H···A)	d(D···A)	∠(DHA)	Symmetry
1					
O(3)–H(3C)···O(1W)	0.85	1.87	2.672(3)	157.7	$-x+1,-y,-z+1$
N(1)–H(1A)···O(3)	0.91	2.41	3.293(5)	163.7	$-x+1,-y,-z+1$
O(1W)–H(1WA)···O(2)	0.849(10)	2.00(2)	2.794(3)	156(4)	x, $y-1$, z
O(1W)–H(1WB)···O(2)	0.850(10)	1.922(14)	2.763(3)	170(4)	$-x+2$, $-y$, $-z$
2					
N(1)–H(1B)···O(6)	0.90	2.09	2.974(2)	165.4	$-x+1$, $y+1/2$, $-z+3/2$
O(4)–H(4A)···O(6)	0.82	1.84	2.650(2)	169.4	$x-1/2$, $-y+1/2$, $-z+2$
O(1)–H(1A)···O(3)	0.82	1.98	2.763(2)	159.5	$x+1/2$, $-y+3/2$, $-z+2$
O(7)–H(7C)···O(3)	0.82	1.97	2.767(2)	162.3	$-x$, $y-1/2$, $-z+3/2$
O(7)–H(7D)···O(4)	0.818(15)	1.974(15)	2.773(2)	165(3)	$-x+1/2$, $-y+1$, $z-1/2$
3					
O(1)–H(1A)···O(6)	0.82	1.88	2.693(3)	172.5	$x+1/2$, $-y+1/2$, $-z+2$
O(4)–H(4A)···O(2)	0.82	1.91	2.721(3)	167.3	$-x+2$, $y+1/2$, $-z+3/2$
O(7)–H(7C)···O(3)	0.85	1.86	2.658(3)	155.8	$x-1$, y, z
4					
O(1)–H(1B)···O(4)	0.82	1.91	2.734(5)	178.2	$x+1$, $y+1$, z
O(4)–H(4A)···O(3)	0.82	1.75	2.567(6)	178.2	$x-1$, y, z
O(8)–H(8B)···O(6)	0.89(2)	1.87(5)	2.723(8)	161(12)	

$$F_0/F = K_q[Q] + 1 \quad (2)$$

where, F_0 and F are the fluorescence intensity in the absence and presence of drug at [Q] concentration, respectively; K_q is the quenching constant and [Q] is the quencher concentration. Plots of F_0/F *vs.* [Q] appear to be linear and K_q depends on temperature.

2.6. *Antioxidant measurements*

2.6.1. Hydroxyl radical scavenging assay. Hydroxyl radicals ($OH^{\cdot}$) in aqueous media were generated through the Fenton system [27]. Complexes **1–4** and HL_3 were dissolved in DMF, whereas HL_1, HL_2, and HL_4 were dissolved in H_2O. The 5 ml assay mixture contained the following reagents: safranin (1 mL, 114 μM), EDTA-Fe(II) (1 mL, 0.945 mM), H_2O_2 (1 mL, 3%), the tested compound (1–10 μM), and a phosphate buffer (2 mL, pH 7.4). The assay mixtures were incubated at 37 °C for 30 min in a water bath, after which the absorbance was measured at 520 nm. All the tests were run in triplicate and are expressed as the mean standard deviation (SD). The suppression ratio for $OH^{\cdot}$ was calculated from the following expression:

$$\text{Suppression ratio } (\%) = (A_i - A_0)/(A_c - A_0) \times 100\% \quad (3)$$

where, A_i = the absorbance in the presence of the tested compound; A_0 = the absorbance in the absence of the tested compound; and A_c = the absorbance in the absence of the tested compound, EDTA–Fe(II).

2.6.2. Superoxide radical scavenging assay. Superoxide radicals ($O_2^{-\cdot}$) were generated *in vitro* by a nonenzymatic system and determined spectrophotometrically by nitro blue tetrazolium (NBT) photoreduction, with a little modification to the method adopted elsewhere [28]. The amount of $O_2^{-\cdot}$ and suppression ratio for $O_2^{-\cdot}$ can be calculated by measuring the absorbance at 560 nm. The tested complexes **1–4** and HL_3 were dissolved in DMF, whereas HL_1, HL_2, and HL_4 were dissolved in H_2O. Solutions of $VitB_2$ and NBT were prepared avoiding light. The assay mixture, in a total volume of 5 ml, contained MET (1 mL, 50 mM), NBT (1 mL, 499.5 μM), $VitB_2$ (1 mL, 33 μM), the tested compound (1–10 μM), and a phosphate buffer (2 mL, pH 7.8). The assay mixtures were incubated at 30 °C for 10 min in a water bath avoiding light, and then, illuminated by a fluorescent lamp for 10 min. After which, the absorbance of the samples (A_i) was measured at 560 nm. The sample without the tested compound was used as control and its absorbance was A_0. All experimental results were expressed as the mean SD of triplicate determinations. The suppression ratio for $O_2^{-\cdot}$ was calculated from the following expression:

$$\text{suppression ratio } (\%) = (A_0 - A_i)/A_0 \times 100\% \quad (4)$$

Drug activity was expressed as the 50% inhibitory concentration (IC_{50}). IC_{50} values were calculated from regression lines where x was the tested compound concentration in μM and y was percent inhibition of the tested compounds.

3. Results and discussion

3.1. *Structures of the copper complexes*

As shown in figure 2, the asymmetric unit of **1** contains one-half of $[Cu(L_1)_2]$ and a lattice water, with Cu(II) on a twofold rotational axis. Copper coordinates to two nitrogens and two carboxylate oxygens from two L_1^- anions, giving a distorted square planar geometry with a N_2O_2 donor set. The Cu–N and Cu–O bond distances are 1.933 and 2.011 Å, respectively. The bond angle of O(1)–Cu(1)–N(1) is 84.50 (10)°.

The structures of **2**, **3,** and **4** are similar. Unlike **1**, Cu^{2+} in **2**, **3,** and **4** coordinates to two nitrogens from two ligand anions and three oxygens, two of which are from two ligand anions and the other is from water, methanol and water, respectively. The coordination geometry was estimated from τ values varying from 0 for an idealized square pyramid to 1 for an idealized trigonal bipyramid [29]. The τ values of **2**, **3,** and **4** are 0.0733, 0.2767, and 0.2985, respectively. (N(1)–Cu(1)–N(2) and O(2)–Cu(1)–O(5) in **2**, **3,** and **4** are 167.14(6) and 171.54(6), 156.15(9) and 172.75(9)°, and 156.34(17) and 174.09(17), respectively. Cu^{2+} in **2**, **3,** and **4** possess coordination geometry closer to distorted square-pyramidal rather than distorted trigonal-bipyramidal. In the five-coordinate structure, the four basal positions are occupied by N(1), N(2), O(2), and O(5). The coordination sphere at the apical position is completed by O7 of water in **2** and **4**, but methanol in **3**. In **4**, the location occupied by C11 is disordered, as C11 and C11a, and both are 0.5. In crystals of **1–4**, there are complicated intermolecular and intramolecular O–H···O interactions, constructing 3D frameworks.

3.2. *Interactions with CT-DNA*

3.2.1. Electronic absorption spectroscopy. Electronic absorption spectroscopy is one of the most useful techniques in examining the binding mode of DNA with metal complexes

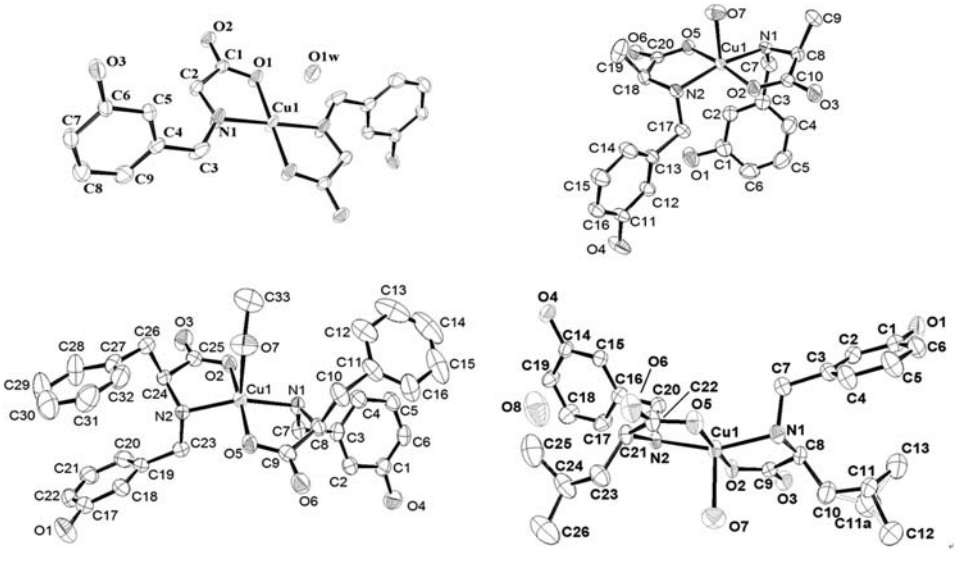

Figure 2. Molecular structures of **1**–**4**. C–H hydrogens are omitted for clarity.

[2]. Intercalative binding usually results in hypochromism and red shift because of the strong stacking interaction between an aromatic chromophore and the base pairs of DNA. The extent of spectral change is related to the strength of binding [30]. Electronic absorption spectra of the ligand and its Cu(II) complexes in the absence and presence of CT-DNA (at a constant concentration of the compounds) were obtained, (figure 3). With increasing DNA concentration, absorption at 274 nm of **1–4** represents hypochromism of 4.89, 14.30, 13.92, and 43.34%, respectively. The hypochromism observed for the π–π^* transitions indicate strong binding of the complexes to DNA. The intrinsic binding constant K_b of **1–4** was 1.32×10^6, 4.32×10^5, 5.00×10^5, and 5.70×10^4 M^{-1}, respectively, which is not in agreement with the hypochromism degree. The K_b values are lower than that reported for the classical intercalator (for ethidium bromide $K_b = 1.4 \times 10^6\,M^{-1}$ and [Ru(phen)DPPZ] with binding constants of 10^6–$10^7\,M^{-1}$) [31–34]. However, they are higher than some reported complexes as shown in table 4. Our results suggest an intimate association of the compounds with CT-DNA and indicate binding strengths of the complexes that follow the order of **1** > **3** > **2** > **4**.

3.2.2. Fluorescence spectroscopy. Fixed amounts (10 μM) of **1–4** were titrated with increasing amounts of CT-DNA; fluorescence titration spectra of the complexes in the absence and presence of CT-DNA are given in figure 4. Compared to the complexes alone, the fluorescence intensity of the complexes is quenched steadily with increasing concentration of CT-DNA. The quenching of luminescence of the complex by DNA may be attributed to photo-electron transfer from the guanine base of DNA to the excited MLCT state of the complex [39–44]. These changes also proved that there were conjugation functions between CT-DNA and the compounds [45, 46].

3.2.3. Competitive DNA-binding studies with EB. In order to further investigate the interaction mode between the complexes and CT-DNA, fluorescence titration experiments were performed. Fluorescence titration experiments, especially ethidium bromide (EtBr) fluorescence competitive experiments, have been widely used to characterize the interaction of complexes with DNA by following the changes in fluorescence intensity of the complexes. The intrinsic fluorescence intensity of EB is low and that of DNA in Tris-HCl buffer is also not high due to the quenching by solvent; fluorescence intensity of EB is enhanced on addition of DNA, because EB intercalates into DNA. The enhanced fluorescence can be quenched when there is a second molecule that can replace DNA-bound EB [47].

As depicted in figure 5, for **1–4** the fluorescence intensity of EB at 601 nm shows remarkable decrease with increasing concentration of the complexes, indicating that some EB molecules are released from EB–DNA after exchange with **1–4**, quenching fluorescence of EB. We assume the reduction of the emission intensity of EB on increasing complex concentration could be due to displacement of DNA-bound EB by the copper(II) complexes [48]. Such quenched fluorescence behavior of EB bound to DNA is also found in other copper complexes [49]. K_q values of **1–4** are 1.516×10^5, 1.913×10^5, 1.436×10^5, and $1.481 \times 10^5\,M^{-1}$, respectively, higher than those of some copper(II) complexes, such as $[Cu_2(oxpep)phen]ClO_4 \cdot (K_q = 9.75 \times 10^4\,M^{-1})$ [50], $[Cu_2(dmeo)(N_3)_2]_n \cdot (K_q = 1.85 \times 10^3\,M^{-1})$ [51], and $[Cu_2L(OAc)(CH_3OH)] \cdot CH_3OH \cdot (K_q = 4.89 \times 10^2\,M^{-1})$ [52]. The data for K_q are in the order **2** > **1** > **4** > **3**, which is not in agreement with the UV–Vis spectroscopy results. Phenolic hydroxyl groups that can bind to nucleotides or/and the sugar–phosphate

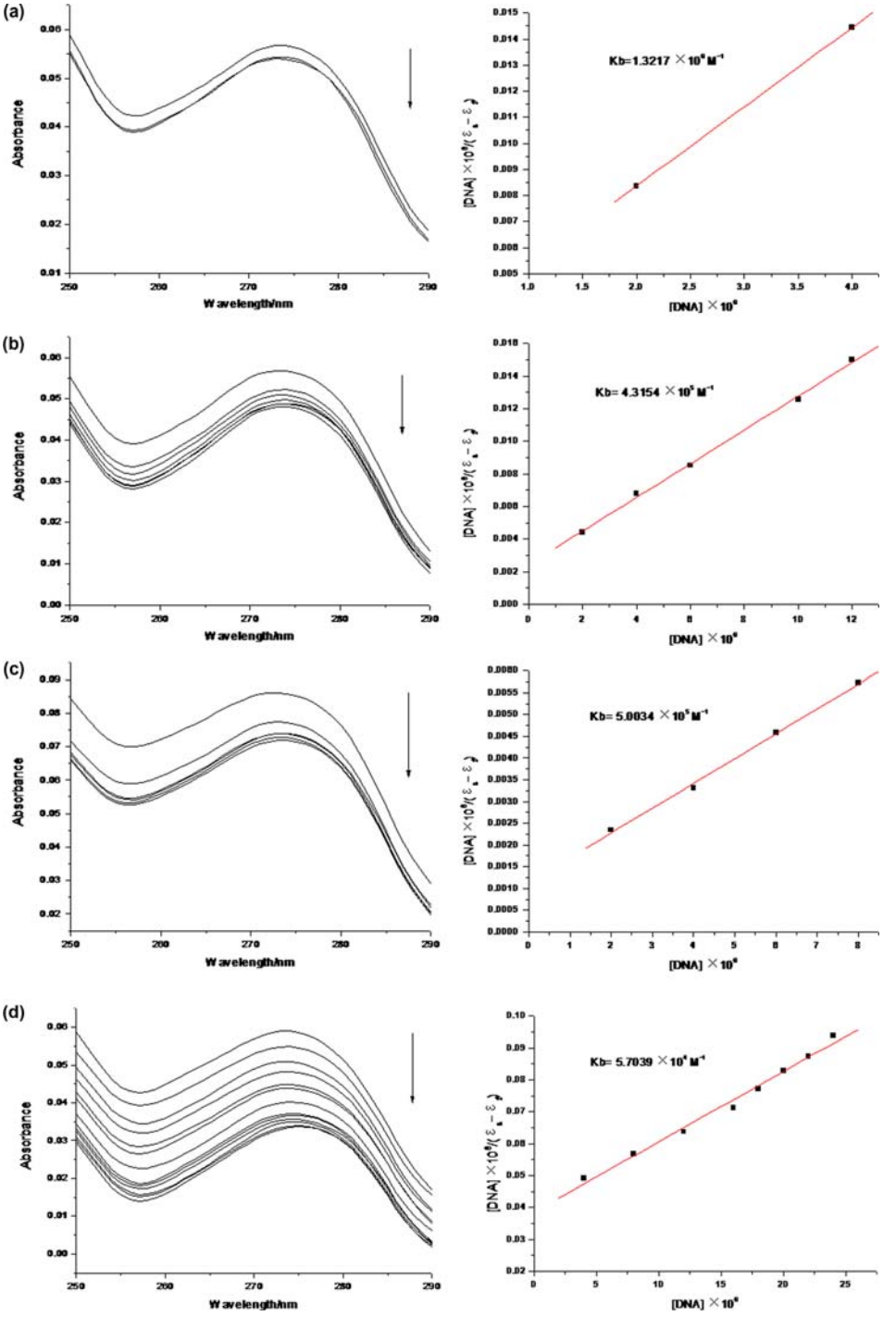

Figure 3. (a), (b), (c), and (d) are the electronic spectra of **1**–**4** (10 μM) in the presence of increasing CT-DNA, respectively. Arrow shows the absorbance changes upon increasing DNA concentration. Inset: Plot of [DNA]/$(\varepsilon_b - \varepsilon_f)$ *vs*. [DNA] for the titration of the Cu(II) complexes with CT-DNA.

Table 4. K_b values of some complexes.

Complex	K_b (M^{-1})	Ref.
[Cu(II)(L^a)(B)]	3.32×10^5	[35]
CuL^b	2.7×10^4	[36]
[Cu(L^c)(bpy)Cl]	1.55×10^4	[37]
[Cu(L^d)phen]$CH_3OH \cdot 0.5H_2O$	4.87×10^3	[7]
$[Cu_2(L^e)_2(H_2O)]$	4.91×10^3	[38]

H_2L^a = salicylidene tryptophan, B = 1,10-phenanthroline.
H_2L^b = Schiff base derived from condensation of 5-nitro-ovanillin and diaminoethane.
HL^c = (E)-3-(2-hydroxyphenylimino)-N-o-tolylbutanamide.
H_2L^d = (E)-2-((2-hydroxynaphthalen-1-yl)methyleneamino)-4-methylpentanoic acid.
H_2L^e = (E)-2-(2-hydroxybenzylideneamino)-4-(methylthio)butanoic acid.

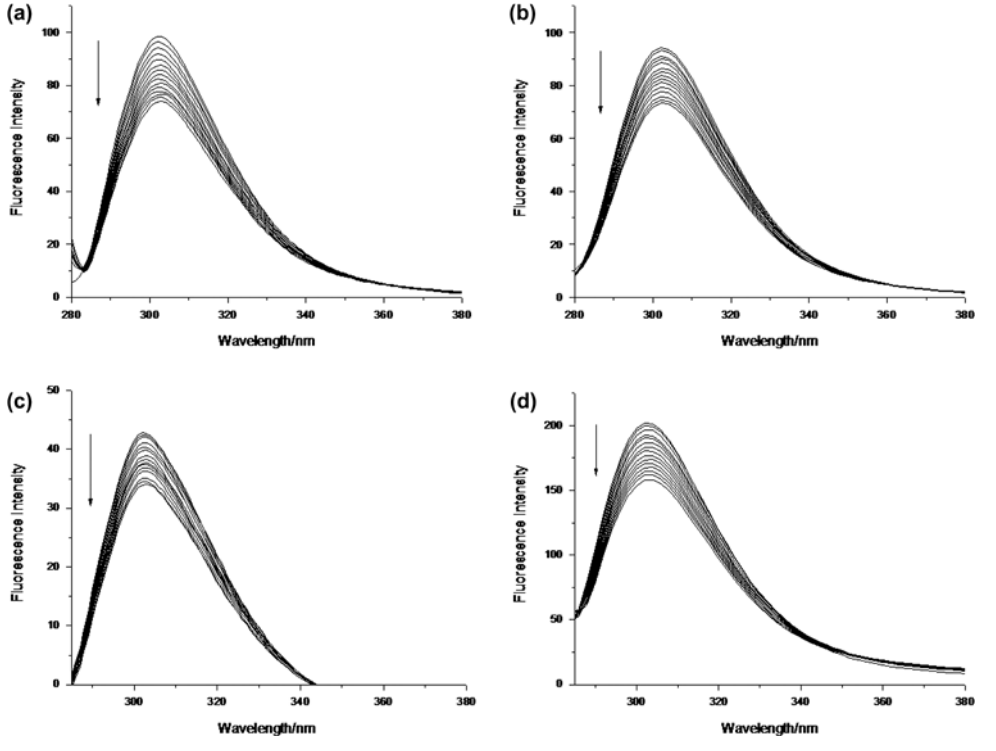

Figure 4. (a), (b), (c), and (d) are emission spectra of **1–4** (10 μM) in the presence of increasing CT-DNA, respectively. Arrow shows the emission intensity changes upon increasing DNA concentration.

backbone of DNA through hydrogen bonds may play roles in the EB–DNA quenching tests. However, other weak interactions such as hydrophobic, van der Waals, and electrostatic forces may not be excluded. The interaction mechanism is not only determined by complex formation but also by weak interactions [53].

3.3. *Hydroxyl radical scavenging activity*

Antioxidant activities of the ligands and their Cu(II) complexes were investigated. The inhibitory effect of the tested compounds on $OH^{\cdot}$ is concentration related and the

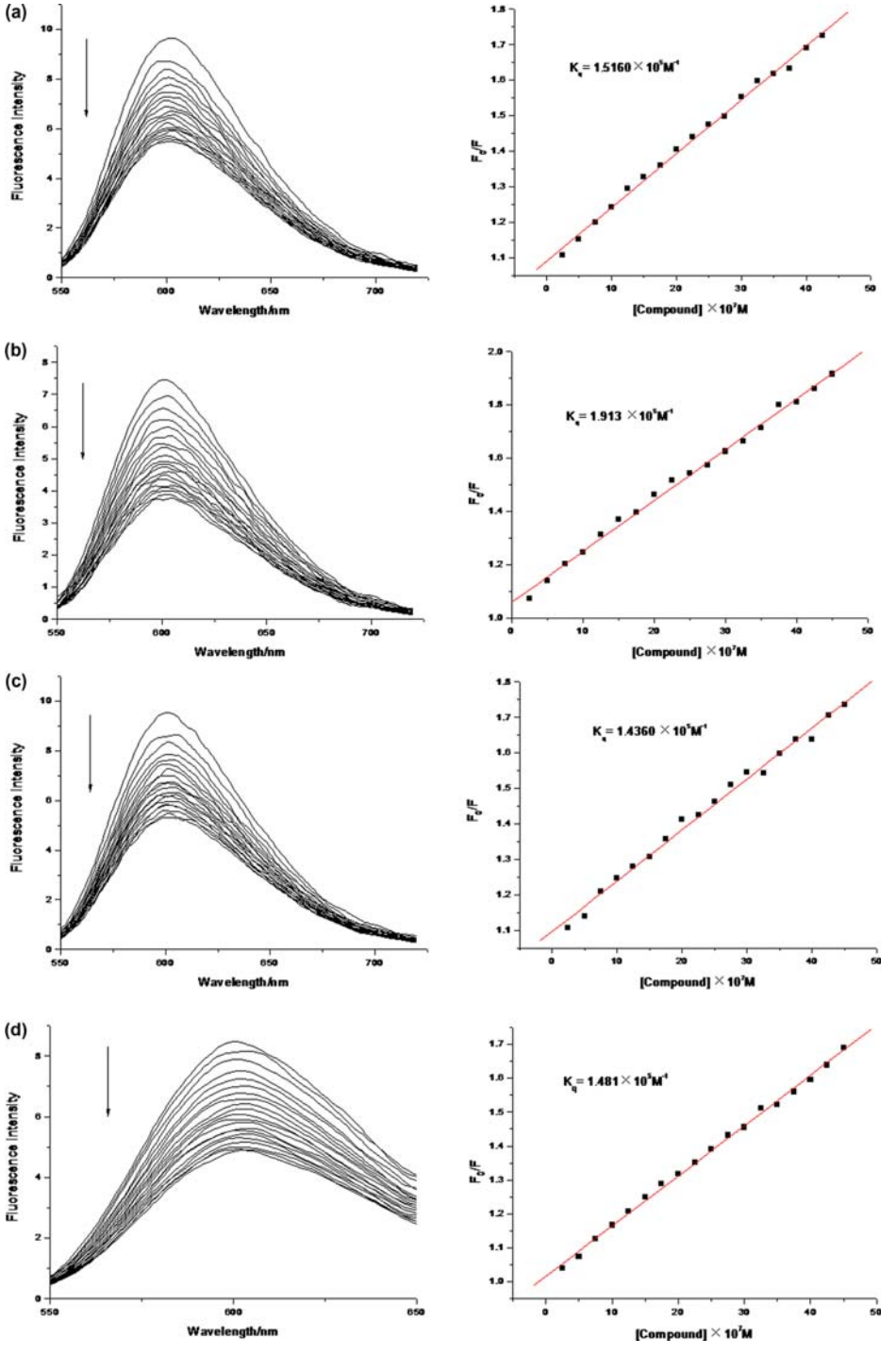

Figure 5. (a) Emission spectra of EB–DNA system in the presence of **1**. Inset: Stern–Volmer plot of the fluorescence titration data of **1**. (b) The emission spectra of EB–DNA system in the presence of **2**. Inset: Stern–Volmer plot of the fluorescence titration data of **2**. (c) The emission spectra of EB–DNA system in the presence of **3**. Inset: Stern–Volmer plot of the fluorescence titration data of **3**. (d) The emission spectra of EB–DNA system in the presence of **4**. Inset: Stern–Volmer plot of the fluorescence titration data of **4**. Arrows show the emission intensity changes upon increasing concentration.

suppression ratio increases with increasing concentration of the sample (figure 6). The IC_{50} values of the ligands cannot be read, while those of **1–4** are 4.61, 4.40, 2.92, and 4.42 μM, respectively. Hydroxyl radical scavenging effects of the Cu(II) complexes are much higher than those of the ligands, possibly from larger conjugated metal complexes reacting with $OH^{\cdot}$ to form larger stable macromolecular radicals [15]. The order of the suppression ratio for $OH^{\cdot}$ is **3** > **2** > **4** > **1**. Usually, mannitol is employed as a standard since it is known to selectively inhibit $OH^{\cdot}$ radical. The IC_{50} values of the complexes are far less than that of mannitol (10.34 μM) [54], however, slightly higher than that of other active compounds and some reported Cu(II) complexes as shown in table 5.

3.4. *Superoxide radical scavenging activity*

The ligands cannot scavenge $O_2^{-\cdot}$ in the tested concentration range. However, the complexes can scavenge $O_2^{-\cdot}$ in a concentration-dependent manner (figure 7). IC_{50} values of **1–4** are 0.04, 0.24, 0.18, and 0.22 μM, respectively, indicating that Cu(II) plays a role in scavenging superoxide. These compounds show higher superoxide dismutase activity than standard antioxidants like vitamin C (IC_{50} = 852 μM) or nitroxide Tempo (IC_{50} = 60 ± 3 μM), which has been recently used in biological systems for its capacity to mimic superoxide dismutase [15]. SOD data for the complexes are compiled in table 6 along with SOD activities of similar complexes containing copper. Complexes **1–4** show higher SOD activity than other similar complexes, but slightly lower than that of native Cu, Zn-SOD [55]. The Cu(II) complexes show similar superoxide dismutase activity comparable with that of native Cu, Zn-SOD. The order of the suppression ratio for $O_2^{-\cdot}$ is **1** > **3** > **4** > **2** at different concentrations, but similar at 0.5 μM. Superoxide radical scavenging activity of **1** is best, probably due to the relatively low coordination number of copper in **1**. The order of the suppression ratio for $O_2^{-\cdot}$ is notably different from the order of suppression ratio for $OH^{\cdot}$, suggesting different mechanisms between scavenging or inhibiting $OH^{\cdot}$ and $O_2^{-\cdot}$, which should be further studied.

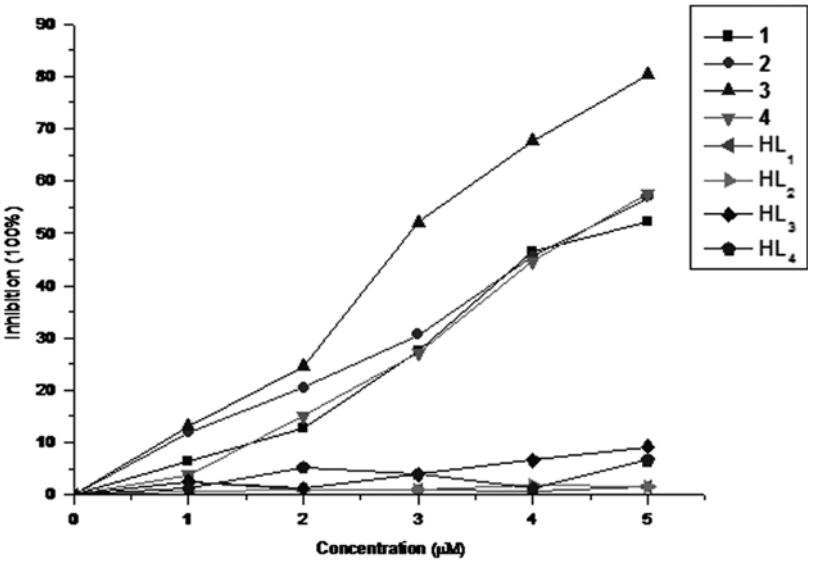

Figure 6. Plots of the hydroxyl radical scavenging effect (%) for ligands and Cu(II) complexes.

Table 5. Hydroxy radical scavenging activity of some copper(II) complexes.

Complex	IC_{50} (μM)	Ref.
Mannitol	10.34	[54]
$[Cu_4(phen)_6(L^f)(H_2O)_2](ClO_4)_6 \cdot 3H_2O$	4.6	[15]
$[Cu_2(phen)_2(L^f)(H_2O)_2](ClO_4)_2 \cdot 2.5H_2O$	5.5	[15]
$[Cu(H_3L^g)]$	<2.5	27[27]
1	4.61	Present work
2	4.40	Present work
3	2.92	Present work
4	4.42	Present work

H_2L^f = N,N′-(p-xylylene)di-alanine acid. phen = 1,10-phenanthroline.
H_5L^g = naringenin-2-hydroxy benzoyl hydrazone.

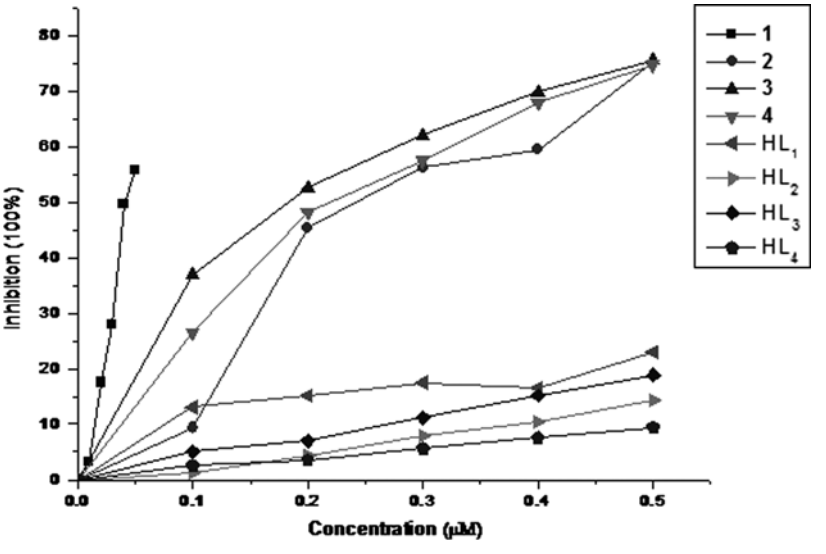

Figure 7. Plots of superoxide radical scavenging effect (%) for Cu(II) complexes.

Table 6. Superoxide dismutase activity of some copper(II) complexes.

Complex	IC_{50} (μM)	Ref.
Native SOD	0.04	[55]
$[Cu(L^h)(bipy)](ClO_4)_2$	105	[56]
$Cu(L^i)_2(L^J)_2$ (1)	0.81	[57]
$[Cu_2(\mu\text{-}L^k)_4(ClO_4)_2](ClO_4)_2 \cdot 2MeOH$	9.24	[58]
$[Cu_2(L^l)(L^m)](ClO_4)_3 \cdot H_2O$	1.42	[59]
1	0.04	Present work
2	0.24	Present work
3	0.18	Present work
4	0.22	Present work

L^h = N,N,N′,N″,N″-pentamethyldiethylenetriamine.
HL^i = aspirinato.
L^J = 2-methylimidazole
L^k = 6-(3-fluorobenzylamino)purine.
HL^l = 6, 20-bis(1H-imidazol-4-ylmethyl)-3, 6, 9, 17, 20, 23-hexaazatricyclo [24,3,1,$1^{11,15}$] hentriaconta-1(29), 11, 13, 15(31), 26(30), 27-hexaene.
L^m = imidazole.

4. Conclusions

Four copper(II) complexes with amino acid ligands were prepared and characterized by single-crystal X-ray crystallography. The Cu(II) complexes bind to CT-DNA through intercalation with binding constants of 10^5–$10^6\,M^{-1}$, and the Cu(II) complexes present stronger affinities to DNA than ligands, showing potential as potential anticancer drugs. The complexes show similar superoxide dismutase activities to that of native Cu, Zn-SOD. Further research is needed to better determine the relationship between structures and activities.

Acknowledgement

This work was supported by the National Science Foundation of China (21001040).

Supplementary data

CCDC 842993–842995 and 873438 contain the supplementary crystallographic data for **1**, **2, 3,** and **4**, respectively. These data can be obtained free of charge from The Cambridge Crystallographic Data Center via www.ccdc.cam.ac.uk/data_request/cif.

References

[1] K.E. Erkkila, D.T. Odom, J.K. Barton. *Chem. Rev.*, **99**, 2777 (1999).
[2] J.K. Barton, A.L. Raphael. *J. Am. Chem. Soc.*, **106**, 2466 (1984).
[3] A. Chouai, S.E. Wicke, C. Turro, J. Bacsa, K.R. Dunbar, R.P. Thummel. *Inorg. Chem.*, **44**, 5996 (2005).
[4] A.M. Pyle, T. Morii, J.K. Barton. *J. Am. Chem. Soc.*, **112**, 9432 (1990).
[5] N. Maribel. *Biol. Inorg. Chem*., **4**, 401 (2003).
[6] S. Arturo, B. Giampaolo, R. Giuseppe, L.G. Maria, T.J. Salvatore. *J. Inorg. Biochem.*, **98**, 589 (2004).
[7] J.F. Dong, L.Z. Li, L.W. Li, T. Xu, D.Q. Wang. *Chin. J. Chem.*, **29**, 259 (2011).
[8] J. Costa Pessoa, M.J. Calhorda, I. Cavaco, I. Correia, M.T. Duarte, V. Felix, R.T. Henriques, I. Tomaz. *J. Chem. Soc.. Dalton Trans.*, 4407 (2002).
[9] R. Karmakar, C.R. Choudhury, S. Mitra, L. Dahlenburg. *Struct. Chem.*, **16**, 611 (2005).
[10] C.T. Yang, B. Moubaraki, K.S. Murray, J.D. Ranford, J.J. Vittal. *Inorg. Chem.*, **40**, 5934 (2001).
[11] C.T. Yang, B. Moubaraki, K.S. Murray, J.J. Vittal. *J. Chem. Soc., Dalton Trans.*, 880 (2003).
[12] P.A.N. Reddy, M. Nethaji, A.R. Chakravarthy. *Eur. J. Inorg. Chem.*, **7**, 1440 (2004).
[13] P.K. Sasmal, A.S. Patra, M. Nethaji, A.R. Chakravarthy. *Inorg. Chem.*, **46**, 11112 (2007).
[14] M.-Z. Wang, Z.-X. Meng, B.-L. Liu, G.-L. Cai, C.-L. Zhang, X.-Y. Wang. *Inorg. Chem. Commun.*, **8**, 368 (2005).
[15] L. Jia, P. Jiang, J. Xu, Z.Y. Hao, X.M. Xu, L.H. Chen, J.C. Wua, N. Tang, J.J. Vittal. *Inorg. Chim. Acta*, **363**, 855 (2010).
[16] I.-ul.-H Bhat, S. Tabassum. *Spectrochim. Acta, Part A*, **72**, 1026 (2009).
[17] V. Uma, M. Kanthimathi, T. Weyhermuller, B.U. Nair. *J. Inorg. Biochem.*, **99**, 2299 (2005).
[18] A.K. Patra, S. Dhar, M. Nethaji, A.R. Chakravarty. *Chem. Commun.*, **1562**, (2003).
[19] P.K. Sasmal, A.K. Patra, A.R. Chakravarty. *J. Inorg. Biochem.*, **102**, 1463 (2008).
[20] R. Rao, A.K. Patra, P.R. Chetana. *Polyhedron*, **27**, 1343 (2008).
[21] L. Jia, N. Tang, J.J. Vittal. *Inorg. Chim. Acta*, **362**, 2525 (2009).
[22] SMART and SAINT Software Reference Manuals, Versions 5.6 and 6.4, Bruker AXS, Madison, WI (2003).
[23] G.M. Sheldrick, SADABS Software for Empirical Absorption Correction, University of Göttingen, Göttingen (2003).
[24] SHELXTL Reference Manual, Version 6.14, Siemens Energy & Automation, Inc., Analytical Instrumentation, Madison, WI (2003).
[25] H. Deng, J.W. Cai, H. Xu, H. Zhang, L.N. Ji. *J. Chem. Soc,. Dalton Trans.*, 325 (2003).
[26] M.R. Eftink, C.A. Ghiron. *Anal. Biochem.*, **114**, 199 (1981).

[27] C.C. Winterbourn. *Biochem. J.*, **198**, 125 (1981).
[28] T.R. Li, Z.Y. Yang, B.D. Wang. *Chem. Pharm. Bull.*, **55**, 26 (2007).
[29] A.W. Addison, T.N. Rao, J. Reedijk, J. van Rijn, G.C. Verchoor. *J. Chem. Soc., Dalton Trans.*, 1349 (1984).
[30] Z.D. Xu, H. Liu, S.L. Xiao, M. Yang, X.H. Bu. *J. Inorg. Biochem.*, **90**, 79 (2002).
[31] M. Cory, D.D. McKee, J. Kagan, D.W. Henry, J.A. Miller. *J. Am. Chem. Soc.*, **107**, 2528 (1985).
[32] M.J. Waring. *J. Mol. Biol.*, **13**, 269 (1965).
[33] V.G. Vaidyanathan, B.U. Nair. *J. Inorg. Biochem.*, **94**, 121 (2003).
[34] R. Vijayalakshmi, M. Kanthimathi, V. Subramanian, B.U. Nair. *Biochim. Biophys. Acta*, **1475**, 157 (2000).
[35] P.R. Reddy, A. Shilpa, N. Raju, P. Raghavaiah. *J. Inorg. Biochem.*, **105**, 1603 (2011).
[36] N. Raman, K. Pothiraj, T. Baskaran. *J. Coord. Chem.*, **64**, 4386 (2011).
[37] K. Pothiraj, T. Baskaran, N. Raman. *J. Coord. Chem.*, **65**, 2110 (2012).
[38] C.Y. Gao, X.F. Ma, J. Lu, Z.G. Wang, J.L. Tian, S.P. Yan. *J. Coord. Chem.*, **64**, 2157 (2011).
[39] R. Vijayalakshmi, M. Kanthimathi, R. Parthasarathi, B.U. Nair. *Bioorg. Med. Chem.*, **14**, 3300 (2006).
[40] P.U. Maheswari, M. Palaniandavar. *J. Inorg. Biochem.*, **98**, 219 (2004).
[41] A.K. Mesmaeker, G. Orellana, J.K. Barton, N.J. Turro. *Photochem. Photobiol.*, **52**, 461 (1990).
[42] J.B. Chaires, N. Dattagupta, D.M. Crothers. *Biochemistry*, **21**, 3933 (1982).
[43] J.Z. Wu, L. Yuan, J.F. Wu. *J. Inorg. Biochem.*, **99**, 2211 (2005).
[44] B. Peng, H. Chao, B. Sun, H. Li, F. Gao, L.N. Ji. *J. Inorg. Biochem.*, **101**, 404 (2007).
[45] P.X. Xi, Z.H. Xu, F.J. Cheng, Z.Z. Zeng, X.W. Zhang. *J. Inorg. Biochem.*, **103**, 210 (2009).
[46] P.X. Xi, Z.H. Xu, X.H. Liu, F.J. Cheng, Z.Z. Zeng. *Spectrochim. Acta, Part A*, **71**, 523 (2008).
[47] H.G. Li, Z.-Y. Yang, B.D. Wang, J.C. Wu. *J. Organomet. Chem.*, **695**, 415 (2010).
[48] Z.Q. Liu, Y.T. Li, Z.Y. Wu, Y.L. Song. *Inorg. Chim. Acta*, **361**, 226 (2008).
[49] U. McDonnell, M.R. Hicks, M.J. Hannon, A. Rodger. *J. Inorg. Biochem.*, **102**, 2052 (2008).
[50] S.H. Cui, M. Jiang, Y.T. Li, Z.Y. Wu, X.W. Li. *J. Coord. Chem.*, **64**, 4209 (2011).
[51] M. Jiang, Y.T. Li, Z.Y. Wu. *J. Coord. Chem.*, **65**, 1858 (2012).
[52] Y. Mei, J.J. Zhou, H. Zhou, Z.Q. Pan. *J. Coord. Chem.*, **65**, 643 (2012).
[53] Y.C. Liu, Z.Y. Yang. *J. Inorg. Biochem.*, **103**, 1014 (2009).
[54] B.D. Wang, Z.Y. Yang, P. Crewdson, D.Q. Wang. *J. Inorg. Biochem.*, **101**, 1492 (2007).
[55] J.L. Pierrs, P. Chatutemps, S. Refait, C. Beguin, A.E. Marzouki, G. Serratrice, P. Rey. *J. Am. Chem. Soc.*, **117**, 965 (1995).
[56] R.N. Patel, N. Singh, K.K. Shukla, U.K. Chouhan, J. Niclos Gutierrez, A. Castineiras. *Inorg. Chim. Acta*, **357**, 2469 (2004).
[57] A.L. Abuhijleh. *Inorg. Chem. Commun.*, **14**, 759 (2011).
[58] A. Klanicová, Z. Trávníček, J. Vančo, I. Popa, Z. Šindelář. *Polyhedron*, **29**, 2582 (2010).
[59] Z.P. Qi, K. Cai, Q. Yuan, T. Okamura, Z.S. Bai, N. Ueyama. *Inorg. Chem. Commun.*, **13**, 847 (2010).